D. L. Morrow and P. Kurath**

Proportional Biaxial-Tension Low Cycle Fatigue of Inconel 718

REFERENCE Morrow, D. L. and Kurath, P., **Proportional biaxial-tension and low cycle fatigue of Inconel 718**, *Biaxial and Multiaxial Fatigue*, EGF 3 (Edited by M. W. Brown and K. J. Miller), 1989, Mechanical Engineering Publications, London, pp. 551–570.

ABSTRACT Axial-torsion test equipment allows the fatigue testing of tubular specimens in stress or strain space quadrants II and IV. Experimental investigations using tubular specimens in quadrants I and III are made possible by combining axial loads with internal and/or external pressure. Previous biaxial-tension experimental techniques and data are reviewed. An initial series of tests was conducted using internal pressure and axial tension on thin-walled tubes. The tests were run in proportional load control with $R_\sigma = 0$ (corresponding to quadrant I of stress space). A second series of tests was conducted with the addition of external pressure and a multiaxial extensometer. This permitted biaxial-tension strain controlled $R_\epsilon = 0$ testing into the plastic range (i.e., quadrant I of strain space).

The materials tested were Inconel 718 and Inconel 718-DA, which has approximately an order of magnitude smaller grain size. Test results for Inconel 718-DA are compared with uniaxial data. Fatigue damage parameters employed in these comparisons are maximum principal strain, maximum principal stress, and a shear strain based parameter. Maximum principal stress provided the most satisfactory correlation for Inconel 718-DA. Adequate correlation of biaxial-tension testing to previous quadrant II and IV biaxial data was achieved for the Inconel 718 by employing a shear strain based parameter. These results indicate that the appropriate damage parameter for biaxial-tension fatigue is material dependent.

Notation

$\sigma_r, \sigma_z, \sigma_\theta$	Radial, longitudinal, and tangential stresses
$\sigma_1, \sigma_2, \sigma_3$	Principal stresses
$\varepsilon_r, \varepsilon_z, \varepsilon_\theta$	Radial, longitudinal, and tangential strains
$\varepsilon_1, \varepsilon_2, \varepsilon_3$	Principal strains
R_σ	Stress ratio, σ_i min/σ_i max
R_ε	Strain ratio, ε_i min/ε_i max
ϕ_σ	Biaxial-tension stress ratio, σ_2/σ_1
ϕ_ε	Biaxial-tension strain ratio, $\varepsilon_2/\varepsilon_1$
t	Specimen thickness
$\overline{\nu}$	Effective Poisson's ratio
ν	Poisson's ratio
E	Young's modulus
P_z	Axial force
P_i	Internal pressure
P_o	External pressure

* Department of Mechanical and Industrial Engineering, University of Illinois at Urbana-Champaign, West Green Street, Urbana, IL 61801, USA.

Introduction

Many components used in the power generation and aircraft industries are subjected to severe multiaxial stresses. The demand for higher engine efficiencies has resulted in increased operating temperatures. In critical applications, e.g., in the design of a turbine disc, these higher temperatures necessitate the use of high strength, creep-resistant, superalloys which exhibit nominally elastic behaviour even at short lives. Major loading cycles, such as ground–air–ground cycles for aircraft engines and start/stop cycles for standby power generation, result in fatigue lives for these materials of approximately 10^3–10^5 cycles.

Fatigue analysis of such components requires the implementation of a multiaxial fatigue theory. A high cycle fatigue (HCF) stress-based approach might be invoked if the material displays nominally elastic behaviour. Alternatively, a crack growth model could be employed which assumes an inclusion or defect to be the initial crack dimension. Finally, low cycle fatigue (LCF) behaviour (defined here as less than 10^5 cycles) has typically been formulated in terms of a strain-based approach.

Biaxial-tension fatigue has been approached via three distinct methodologies: high cycle fatigue, using stress-based fatigue theories; low cycle fatigue, using strain-based fatigue theories; and crack growth. These approaches represent different life regimes and possibly different failure mechanisms. The somewhat arbitrary definitions of crack initiation proposed by various researchers may cause the initiation and small crack propagation approach of low cycle fatigue to overlap the long crack propagation approach. Thorough reviews of specimen designs, loading apparatus, and damage evaluation techniques are available in the literature (**1**)–(**6**). A few representative works will be discussed here.

High cycle fatigue

Most early researchers found stress-based fatigue criteria to be most applicable to multiaxial fatigue analysis when observed cyclic plastic strains were orders of magnitude smaller than the elastic strains. These stress-based criteria are extensions of static yield theories such as the maximum normal stress, maximum shear stress, etc., which are primarily limited to high cycle fatigue analysis (**3**).

With regard to biaxial-tension fatigue, the work of Blass and Findley (**7**) on an AISI 4340 thick-walled steel tube (t = 5.3 mm) shows essentially no difference in fatigue life for equal biaxial-tension loading ($\phi_\sigma = 1$) and uniaxial loading ($\phi_\sigma = 0$) for a life slightly greater than 10^5 cycles. Data were presented as maximum principal shear stress versus log life. The work of Bundy and Marin (**8**) on the biaxial fatigue strength of 14S-T4 aluminium thin-walled tubes (t = 1.3 mm) from 10^4 to 10^7 cycles also indicated that fatigue characteristics at long life for equal biaxial-tension and uniaxial loading cases are similar. These

data were presented as maximum principal stress versus cycles to failure; they revealed essentially the same Basquin coefficients and exponents for the *S–N* curves. An attempt to correlate test data using a modified energy theory met with poor results.

Low cycle fatigue

Most researchers involved in LCF have employed strain-based parameters to present their data. As in high cycle biaxial fatigue, many LCF criteria are extensions of strain-based yield/failure criteria such as maximum normal strain, maximum shear strain, etc. There are additional complexities involved in LCF analysis, namely, the determination, either analytically or experimentally, of the path dependent cyclic plastic deformation. Cyclic deformation must be understood in order to formulate the correct stress–strain response which can then be evaluated by a given failure criterion.

Pascoe and de Villiers (**9**) tested mild steel and QT35 steel, using cruciform specimens with a gauge section thickness of 1 mm. Three biaxial-tension strain ratios were tested and resulted in shear loading ($\phi_\varepsilon = -1$), uniaxial loading ($\phi_\varepsilon = 0$), and equal biaxial loading ($\phi_\varepsilon = 1$). Choice of strain levels resulted in fatigue lives of 10^2–10^4 cycles. These tests were performed in load control with the cyclic limits being determined by strain gauges located in the gauge section. Data were presented as log maximum principal strain range versus log life. Equal biaxial-tension loading reduced the allowable strain range by 50 per cent at 10^3 cycles, in comparison to the uniaxial loading case. No parameter to correlate their data was proposed.

Havard *et al.* (**10**)–(**12**) tested normalized 1018 steel thin-walled tubes (t = 1.1 mm and t = 0.5 mm). Six ratios of axial to hoop stress (different from biaxial-tension stress ratio), σ_z/σ_θ, ranging from +3.89 to −3.63 were achieved by varying specimen geometry and nominal loading. Gauge section extensometry was used to monitor diametral and axial strain. Two specimen geometries were required to achieve the range of stress ratios tested. Experimental fatigue lives ranged from 2×10^3 to 10^5 cycles, and data were presented as log maximum principal strain range versus log life. A comparison of the uniaxial with equal biaxial-tension data in the form of principal total strain range at 10^3 cycles indicated that the biaxial-tension loading case reduced the allowable strain range 70 per cent from that of the uniaxial case. Originally, a modified maximum shear-stress criterion (**10**)(**11**) was proposed to correlate the data. The scatter in fatigue life was reduced to within a factor of 5. This damage model was later changed to an octahedral shear strain criterion modified by the hydrostatic stress (**12**).

Andrews and Ellison (**13**)(**14**) tested RR58 aluminium alloy thin-walled tubes with a gauge section thickness of 1.0 mm. Improved gauge section extensometry, specimen design, and control systems allowed surface biaxial-tension strain ratio control (ϕ_ε) over the entire range of biaxiality. Data for

fatigue lives ranging from 10^2 to 6×10^3 cycles were presented as log maximum principal strain amplitude versus log life. The biaxial-tension strain ratio of $\phi_\varepsilon = +1$ was shown to be the most damaging. The maximum principal strain amplitude for a 10^3 cycle life was 40 per cent less than in the uniaxial loading case. A von Mises equivalent strain function was proposed as the failure criterion, which was then modified by allowing an effective Poisson's ratio, $\bar{\nu}$, to vary between elastic and fully plastic values. The value of $\bar{\nu}$ was dependent on strain range.

Lohr and Ellison (**15**)(**16**) tested 1 Cr–Mo–V steel thin-walled tubes with a gauge section thickness of 1.0 mm. Significant improvements on Andrews' (**13**) test facility resulted in increased range and accuracy of strain measurement and control capabilities. Here, specimen fatigue lives ranged from 500 to 10^4 cycles, and data were presented as log maximum principal strain amplitude versus log life. The biaxial-tension strain ratio of $\phi_\varepsilon = +1$ was again shown to be the most damaging, with the principal strain amplitude for a life of 10^3 cycles being 44 per cent less than the uniaxial for the same life. A simplified theory of LCF multiaxial failure was proposed which was similar to the maximum shear strain critical plane theory proposed by Brown and Miller (**5**) with an important exception: maximum shear and normal strains on planes 45 degrees to the surface were always assumed to dictate crack growth through the specimen thickness and thereby control the fatigue life. For biaxial-tension loading, the two theories are identical, whereas differences exist concerning principal stress or strain quadrants II and IV.

LeFebvre *et al.* (**17**) tested A-516 low alloy steel thin-walled tubes with a gauge length thickness of 0.75 mm and 0.5 mm for negative and positive strain ratios, respectively. Seven ratios of hoop to axial strain (different from biaxial-tension strain ratio), $\varepsilon_\theta/\varepsilon_z$, from -1.25 to $+1.0$ were investigated under fully reversed strain control ($R_\varepsilon = -1$). Data for fatigue lives ranging from 300 to 10^5 cycles were presented as log stress or strain amplitude versus log life. Again, the biaxial-tension strain ratio of $+1$ was the most damaging; the total principal strain amplitude for a life of 10^3 cycles was 77 per cent lower than the axial case.

Crack growth

Investigations of fatigue crack propagation under biaxial loading are commonly performed on cruciform specimens under load control. This specimen configuration allows for observation of the crack on both specimen surfaces. Stresses and strains at the crack tip are readily calculated employing the finite element method. Fracture mechanics concepts can be used to quantify damage and estimate lives for components.

Charvat and Garrett (**18**) tested mild steel cruciform specimens with a center section thickness of 6 mm and a 14 mm centre starter notch. The three biaxial-tension stress ratios investigated were $\phi_\sigma = +1, 0$, and -1 at a load ratio $R_\sigma = 0$. Charvat found that $\phi_\sigma = -1$ (compressive transverse stresses)

accelerated crack growth, whereas $\phi_\sigma = +1$ (equal biaxial-tension) slowed crack growth with respect to the uniaxial crack growth rate. These conclusions were strengthened by changeover tests, where the stress ratio was changed during the tests and subsequent crack growth rate observed. Charvat noted that the design of his test apparatus eliminated bending induced by cross-axis loading and the anisotropy due to the presence of the crack. This fixture was proposed to better represent the effects of biaxial-tension loading.

Hoshide *et al.* (**19**) tested structural low carbon steel cruciform specimens with a centre section thickness of 2 mm and a 1 mm centre starter notch. Three biaxial-tension stress ratios, $\phi_\sigma = +1, 0$, and -1, were tested at load ratios $R_\sigma = 0$ and $R_\sigma = -1$ (i.e., zero to maximum and completely reversed loading, respectively). Maximum stresses were the same for all tests and resulted in the $R_\sigma = -1$ tests having shorter lives than the $R_\sigma = 0$. The $R_\sigma = -1$ tests revealed the same effect of biaxiality on crack growth rate as observed by Charvat, namely, $\phi_\sigma = -1$ accelerated crack growth while $\phi_\sigma = 1$ retarded crack growth relative to the uniaxial case. For $R_\sigma = 0$, the results indicated $\phi_\sigma = 1$ and $\phi_\sigma = -1$ slowed crack growth relative to fully reversed testing, with $\phi_\sigma = -1$ having the slower growth rate. This decrease in crack propagation rate was attributed to the plastic stretching that occurred on the initial cycles.

Brown and Miller (**20**) tested AISI 316 stainless steel cruciform specimens with a centre section thickness of 4 mm and 4 mm centre starter notch. The biaxial-tension stress ratios investigated were $\phi_\sigma = +1, 0$, and -1; except for threshold tests, all tests were conducted at a load ratio $R_\sigma = -1$ to avoid ratchetting. Careful design of a unique specimen resulted in a very uniform stress distribution without cross-axis sensitivity or induced bending. Results over a wide range of loads agreed with earlier findings that the shear loading case, $\phi_\sigma = -1$, increased crack growth rates while the $\phi_\sigma = +1$ loading slowed growth rates relative to the uniaxial case. A crack growth equation was proposed based on the crack tip severe-strain zone size.

Discussion of previous research

As can be seen in the preceding brief review of HCF, LCF, and crack growth approaches, multiaxial fatigue analysis is complex and, at first glance, full of inconsistencies. For example, when compared to uniaxial data, the biaxial-tension fatigue data indicate little or no difference in fatigue life for HCF, severe decrease in fatigue life for LCF, and a markedly decreased crack growth rate. This suggests that the material dependent damage mechanisms responsible for nucleating and growing cracks to failure for LCF may differ from those in effect for HCF and long crack growth. Therefore, even for analysis limited to principal stress quadrant I, no single approach can be applied over the entire life range.

Specimen geometry plays an important role in interpreting data. For example, the critical dimension for initiation and short crack propagation tests on tubes with internal pressure is obviously the gauge section thickness

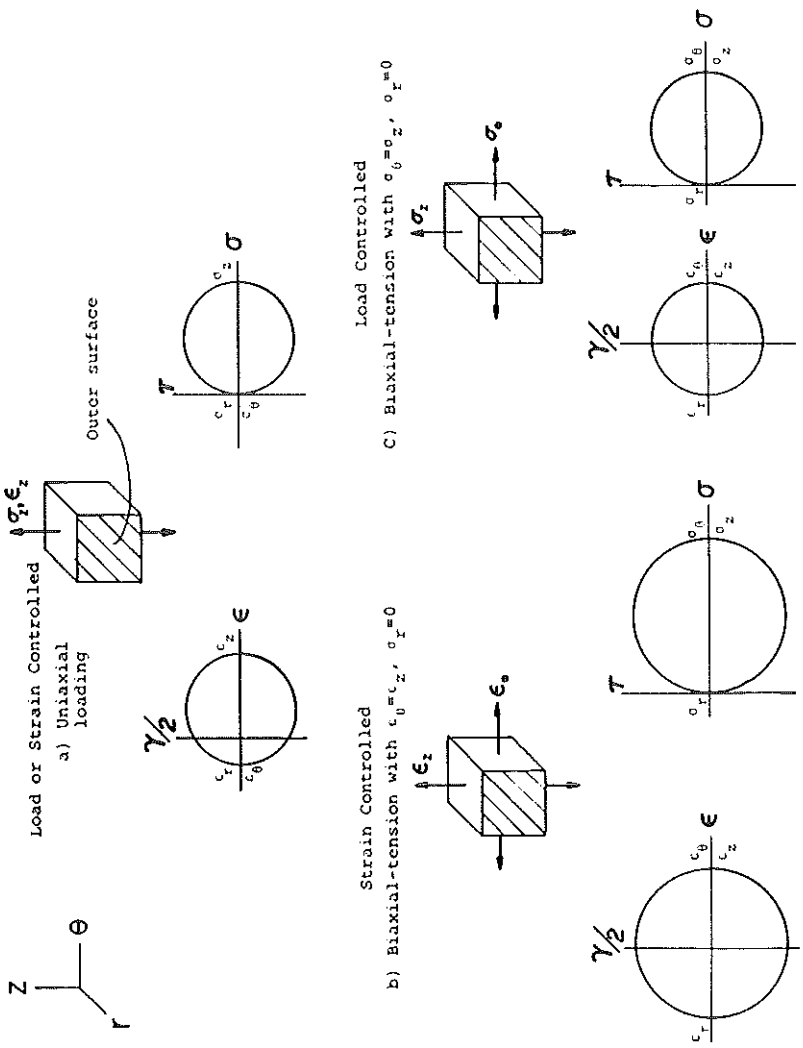

Fig 1 Uniaxial and biaxial tension loadings with resulting Mohr's circles of stress and strain

(typically 1 mm), since a crack through the thickness will cause leakage and terminate the test. The final crack lengths for HCF and LCF studies are approximately the same as the 1 to 5 mm starter notch in a cruciform specimen used for long crack growth studies. The use of crack growth data from large cracks to predict crack growth from small inclusion-sized cracks has been shown to be inappropriate. Most specimen designs for biaxial-tension fatigue research must compromise uniform stress distribution to some degree in order to eliminate buckling failure. Some researchers therefore employ several specimen designs to cover a wide range of biaxial-tension stress or strain ratios. This introduces additional complexities in analysing the data, since geometry effects such as bending are different for each specimen design.

Another interesting and often overlooked factor in comparing biaxial-tension HCF, LCF, and crack growth data to uniaxial data is the difference in stress or strain response during load controlled versus strain controlled tests. HCF and crack growth tests are primarily load/stress controlled, while LCF tests are strain controlled. Figure 1(a) shows a surface element under elastic uniaxial loading in either stress or strain control with the resulting Mohr's circles of stress and strain. If an equal biaxial-tension test is performed in strain control using the value of ε_z obtained from the uniaxial case (Fig. 1(b)), considerably higher shear stress or strain occurs. Applying the theory of elasticity with $\varepsilon_z = \varepsilon_\theta = \varepsilon_{\text{uniaxial}}$, then $\varepsilon_r = -2\nu\varepsilon_z/(1-\nu)$. Calculations of the anticipated stress responses are $\sigma_z = \sigma_\theta = \varepsilon_z E/(1-\nu)$, $\sigma_r = 0$ or $\sigma_z = 1.4\sigma_{\text{uniaxial}}$. Figure 1(b) shows this dramatic increase in shear strain. The von Mises equivalent strains also vary from those calculated for the uniaxial test.

If, on the other hand, an equal biaxial-tension test is performed in load control with the value σ_z from the uniaxial case (Fig. 1(c)), such that $\sigma_z = \sigma_\theta = \sigma_{\text{uniaxial}}$ and $\sigma_r = 0$, then from elasticity $\varepsilon_z = \varepsilon_\theta = \sigma_z(1-\nu)/E$ and $\varepsilon_r = -2\nu\sigma_z/E$. The resulting Mohr's circle of strain shown in Fig. 1(c) indicates a reduction in maximum principal strain, while the maximum shear strain amplitudes and von Mises equivalent strains are identical to those calculated for uniaxial loading.

Keeping Fig. 1 in mind, it is easy to understand why an equal biaxial-tension strain controlled (LCF) test would appear more damaging when compared to the same uniaxial strain. One could also rationalize why a biaxial-tension load controlled test (HCF) would differ little in fatigue life and possibly even benefit from the reduction of normal strains to the maximum shear plane when compared to the uniaxial case.

Purpose and scope of present work

Complexities and expenses involved in performing fatigue tests in stress or strain quadrants I and III are enormous. Therefore, relatively little experimental work has evaluated material fatigue characteristics for these loadings. The purpose of this research is to characterize the fatigue behaviour of two Inconel alloys under biaxial-tension loading. This is part of an even broader overall

program undertaken to ascertain the multiaxial fatigue behaviour of high strength alloys.

Material properties and the stress state required for testing play a major role in specimen selection. These Inconel alloys require high stress levels to obtain life regimes of 10^5 cycles or less. The critical location experiencing fatigue damage in an actual component is often a small region constrained by lower stress state material. This corresponds to a strain controlled laboratory situation to which tubular specimens are well suited. Although the volume of material in the gauge section of the test specimen is greater than that in the typical component, the resultant fatigue life should be conservative. A cruciform specimen without a starter notch requires the analytical calculation of nominal loads to correspond to component strains in the gauge section. For the strain excursions of interest (i.e., zero to max. biaxial-tension loading), the cruciform specimen could experience ratchetting uncharacteristic of the component.

To preserve the polycrystalline behaviour of these high strength materials, the wall thickness of the tube should be 10 or more grain diameters (~1 mm). Loading capabilities of the internal/external pressure system combined with the required 1 mm wall thickness dictate a specimen diameter of approximately 25 mm to achieve the desired stress levels. Failure cracks 1–2 mm in length result from the choice of geometry and correspond to the growth of a crack through the wall thickness. The low fracture toughness of these high strength materials, in conjunction with the high stress levels desired, result in critical crack sizes marginally larger than the failure crack size of the tubular specimen. Fatigue lives obtained from either tubular or unnotched cruciform specimens should not differ substantially, based on final crack size.

A new test system was commissioned to perform biaxial tests in any strain quadrant on thin-walled tube specimens. An overview of the system and its capacities are presented. Biaxial-tension test data from two Inconel 718 alloys are compared to existing data from strain quadrants II and IV employing several multiaxial fatigue theories.

Experimental equipment and testing programme

A new multiaxial testing system was developed jointly by MTS Corporation and the University of Illinois at Urbana-Champaign. This system has the capability of loading a tube specimen in any stress or strain quadrant through various applications of tension/compression, torsion, and internal and external pressure. The system is rated as follows:

Tension load = 445 kN (100 kip)
Compression load = 1112 kN (250 kip)
Internal pressure = 138 MPa (20 ksi)
External pressure = 138 MPa (20 ksi)
Torsion = 5650 kN mm (50 in-kip)

Dow 550 silicon oil is the fluid used for internal and external pressure.

An MTS model 632.85B-11 extensometer was modified to measure axial, torsional, and diametral displacements at pressures to 138 MPa. This was used to perform direct gauge section strain control tests. The extensometer is linear in all three degrees of freedom to within ±1/2 per cent over the full range.

The specimens used in the biaxial-tension tests were thin-walled tubes with a 25 mm bore and a gauge section outside diameter of 28 mm (Fig. 2). The finite element method was employed to investigate the elastic stress–strain response of the tube specimen to help identify the critical stress–strain location. Modelling of the $\phi_\sigma = 0.93$ biaxial-tension loading condition was accomplished by employing elastic eight-noded, axisymmetric-isoparametric elements arranged as shown in Fig. 3. Symmetry of loading and specimen geometry allow only half the specimen to be modeled. Hoop stresses due to pressure loading are nearly constant in the gauge section. However, the axial stress resulting from either axial loading or internal pressure exhibits a slight peak (~5 per cent increase) at the transition from the gauge section to the shoulder, but is constant within the gauge section. This stress rise is due to bending induced by the shoulder

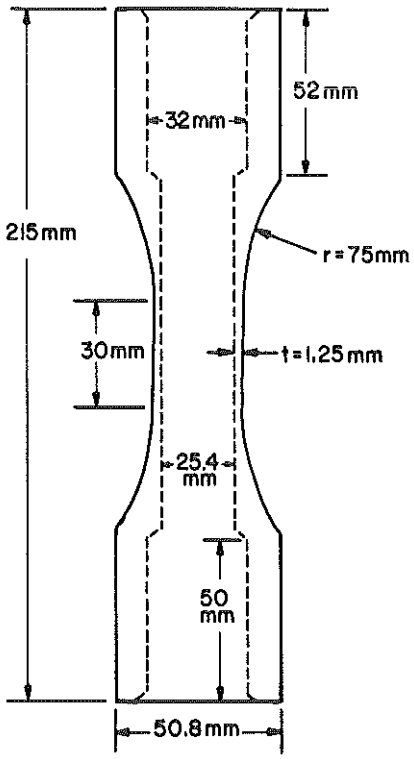

Fig 2 Biaxial-tension specimen

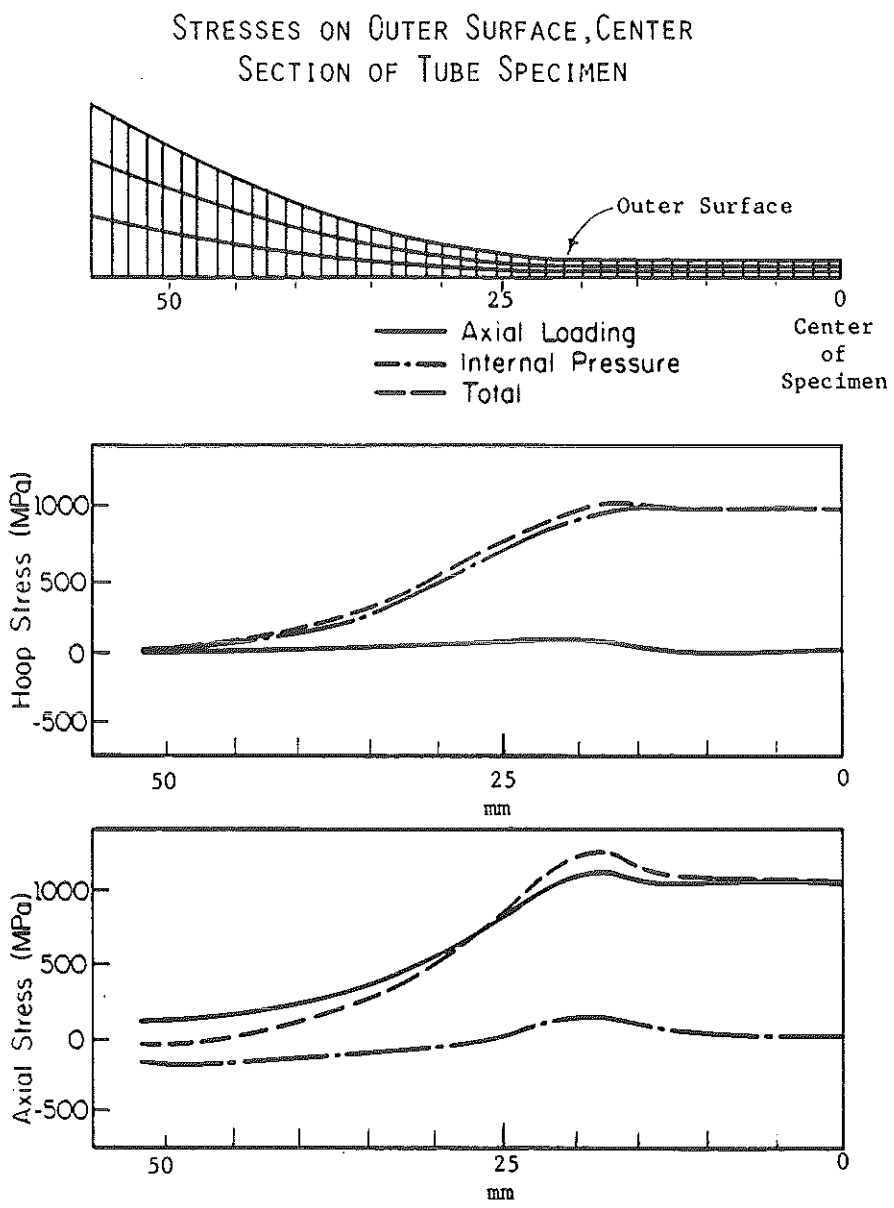

Fig 3 Centre section mesh and elastic finite element results

material. A similar phenomenon was noted for this specimen type by Andrews (**13**). Pressure induced bending reduced the inner surface axial stress to approximately 92 per cent of the outer surface axial stress value. Thick-walled tube constraints reduced the outer surface hoop stress to approximately 93 per cent of the inner surface hoop stress. The highest stressed region occurred on

the outer surface at the location of the peak indicated in Fig. 3. The stress response indicated by this model is employed to assess fatigue damage for failures noted at this location.

The specimen was gripped with precision machine collets, thereby eliminating the requirement for threads on the specimen while maintaining excellent alignment. A mandrel was used to decouple the stresses and strains produced by internal pressure from the axial loading system. This allowed more direct control of the principal stresses or strains.

Two Inconel 718 nickel-based superalloys were investigated. An Inconel 718 and Inconel 718-DA were tested with the Inconel 718 grains being randomly oriented and ranging from 0.01 to 0.2 mm, as shown in Fig. 4. The Inconel 718-DA has approximately an order of magnitude smaller grain size. All biaxial-tension tests were conducted at $R_\varepsilon = 0$ or $R_\sigma = 0$. Baseline uniaxial data were generated on smooth specimens machined to ASTM E606 recommendations, with a gauge length of 25.4 mm and a diameter of 6.4 mm. Tests were

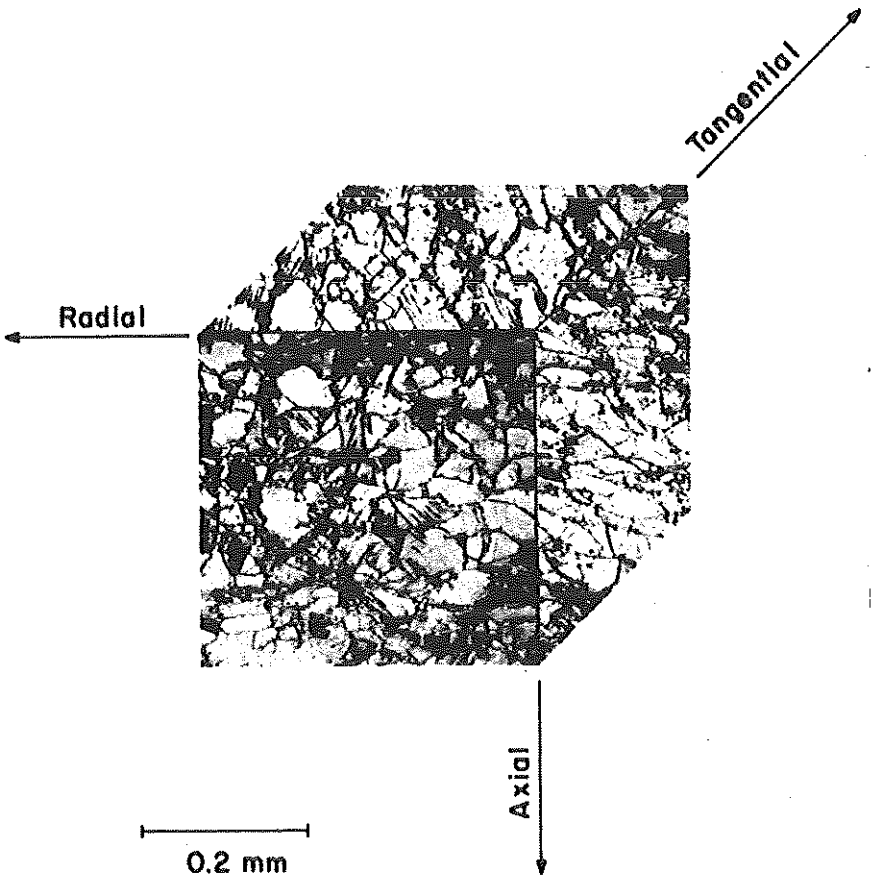

Fig 4 Etched microstructure for the coarse grained Inconel 718

Table 1 Biaxial-tension test data

IN 718-DA

	Control parameters						*Stable half life values*			
	ε_z		ε_θ		$P_z(kN)$		$P_i(MPa)$			
Specimen	*max*	*min*	*max*	*min*	*max*	*min*	*max*	*min*	P_o *(MPa)*	N_f *(cycles)*
08	0.004	0	0.0036	0	113.1	−6.6	132.9	15.7	34.5	30786
09	0.006	0	0.0032	0	130.5	−33.8	127.6	7.6	27.6	20250
10	0.006	0	0.0032	0	128.3	−14.2	124.1	5.5	27.9	17330

	Control parameters					
	$P_z(kN)$		$P_i(MPa)$			
Specimen	*max*	*min*	*max*	*min*	$P_o(MPa)$	$N_f(cycles)$
05	110	0	98.3	0	0	42280
06	110	0	98.3	0	0	26370

IN 718

	Control parameters					
	$P_z(kN)$		$P_i(MPa)$			
Specimen	*max*	*min*	*max*	*min*	$P_o(MPa)$	$N_f(cycles)$
01	110	0	98.3	0	0	30790
02	110	0	98.3	0	0	35910

performed under strain control with $R_\varepsilon = 0$. Tube specimen tests under axial loading with $R_\varepsilon = 0$ displayed fatigue lives similar to the smooth specimens. This indicates that, for this material, geometry effects are negligible when comparing the uniaxial smooth specimen data to axial tube data. Table 1 lists the conditions and results for the Inconel 718-DA and 718 biaxial-tension tests. Two stress controlled tests were performed employing the coarse grained Inconel 718 specimens. Stress strain response for these tests was elastic. Failure occurred at a location corresponding to $\phi_\sigma = 0.93$ (i.e., at the transition from gauge section to specimen shoulder). For the fine grained 718-DA, three strain controlled and two stress controlled tests were performed. The stress controlled tests (Spec. Nos 05 and 06) were elastic with $\phi_\sigma = 0.93$. The strain controlled tests (Spec. Nos 09 and 10) with $\phi_\varepsilon = 0.53$ exhibited initial plasticity followed by elastic cyclic behaviour. The stress-strain response for a strain controlled test (Spec. No. 09) is shown in Fig. 5(a). The observation that zero strain does not occur at zero stress indicates that some initial plastic deformation occurred, while the cyclic response is macroscopically elastic. The principal strains for this test are in phase and proportional, as indicated in Fig. 5(b). The $\phi_\varepsilon = 0.91$ (Spec. No. 08) test is a strain control test intended to duplicate $\phi_\sigma = 0.93$ conditions.

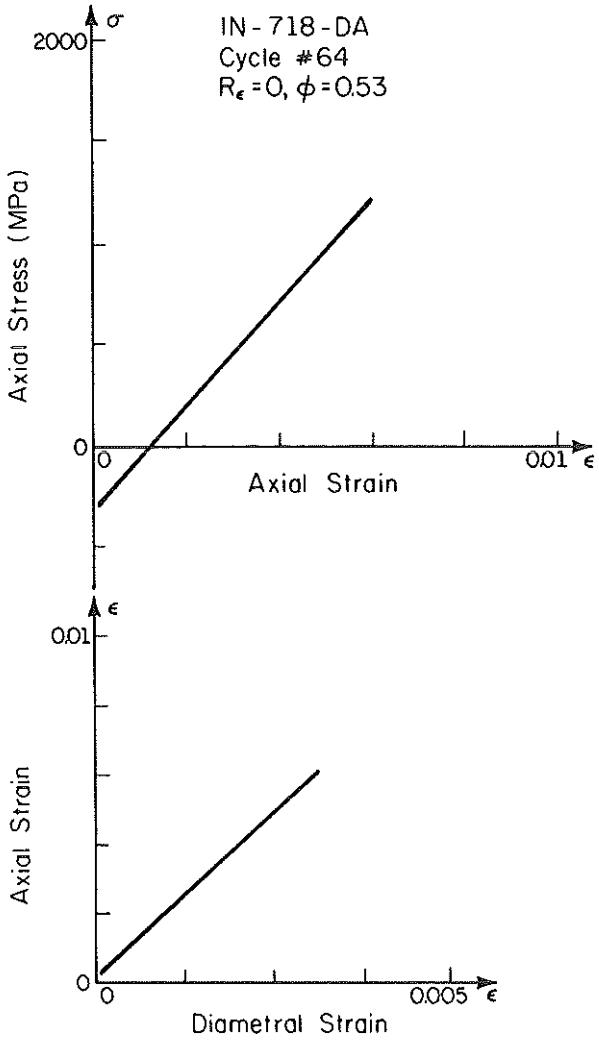

Fig 5 Typical biaxial-tension axial stress strain and axial diametral strain response for Inconel 718-DA specimen No. 09

Discussion

Failure for the biaxial-tension tests was defined to occur when a crack grew through the specimen thickness, causing loss of pressure control. Cracks were typically 1–4 mm long on the surface using this failure criterion. A representative biaxial-tension fatigue crack is shown in Fig. 6. This specimen was tested under $\phi_\sigma = +1$ on the gauge section inside surface. The failure occurred at the transition of the gauge section to the specimen shoulder and initiated from the outer surface. The lack of a definite surface crack direction is attributed to the

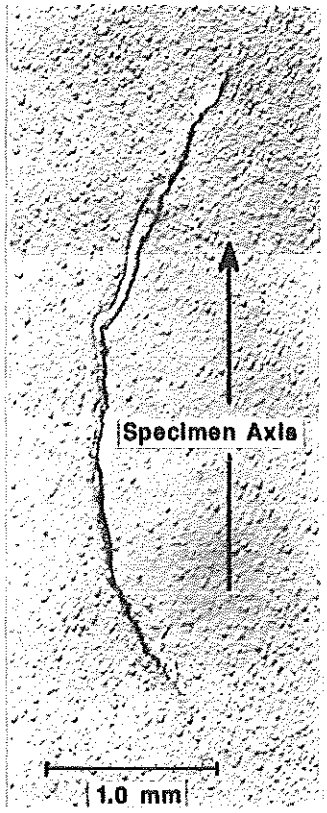

Fig 6 Representative failure crack for Inconel 718-DA under biaxial-tension loading with $\phi_\sigma \approx 0.93$

nearly equal biaxial-tension stress state. The finite element model (Fig. 3) predicts a $\phi_\sigma = +0.93$ stress state at this location and an increased axial principal stress amplitude.

Figure 7 presents the Inconel 718-DA data as log maximum principal strain amplitude at the failure location versus log life. Though there are insufficient data to complete the biaxial-tension curve, it is observed that the $\phi \simeq +1$ loading reduced the allowable strain amplitude by approximately 45 per cent at 3×10^4 cycles. At $\phi_\varepsilon \simeq 0.5$ the reduction in allowable strain is 25 per cent at 2×10^4 cycles. The maximum principal strain parameter does not adequately correlate the biaxial-tension loading to other strain states for this material. Life estimates would be nonconservative employing this damage criterion. Increased stress for biaxial-tension loadings in comparison to other strain quadrants for similar principal strains may be the reason why this damage parameter is inappropriate. The improved correlation of $\phi_\varepsilon \simeq +0.5$ data, where this deformation phenomenon is less than that for $\phi_\varepsilon \simeq 1$, substantiates this premise.

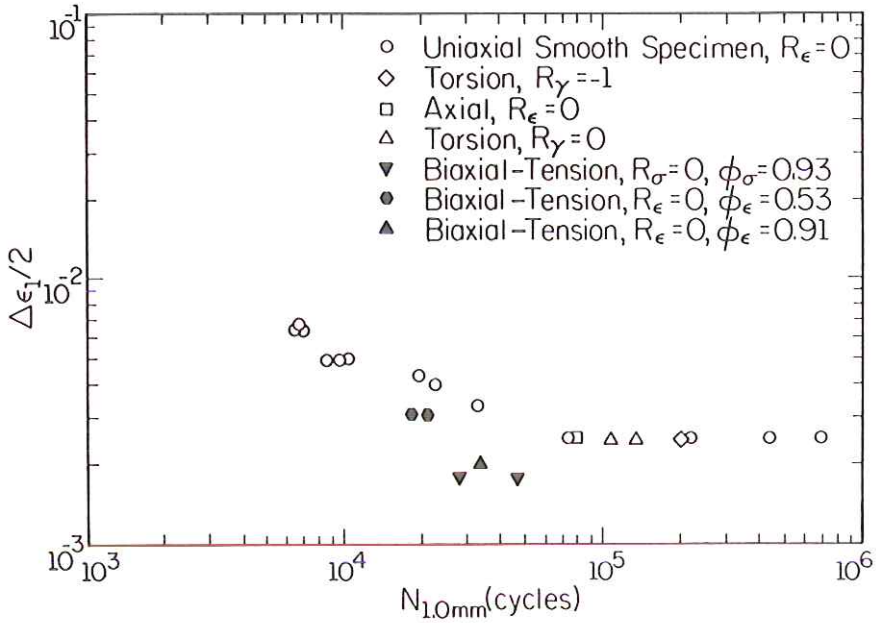

Fig 7 Principal strain amplitude correlation of Inconel 718-DA data

The plot of log maximum principal stress amplitude versus log life shown in Fig. 8 demonstrates a good correlation for $\phi_\varepsilon \simeq 0.5$ data, while the $\phi = +1$ life correlation is within a factor of 4. The failure location for the data presented was at the outer surface where $\sigma_3 = 0$; therefore, the maximum principal stress criteria will offer the same correlations as the maximum shear strain or effective strain parameter. The improved correlation with this parameter further substantiates the notion that stress response should be included in a general damage formulation for the Inconel 718-DA. Since all tests conducted display elastic cyclic deformation, it remains unclear if stress alone is an adequate parameter.

Socie *et al.* (**21**) proposed a mean stress modification to Brown and Miller's (**5**) shear strain based theory for multiaxial fatigue failure. The modified theory still assumes, however, that maximum shear strains are important in dictating cracking direction, but allows both strains and stresses normal to the plane of maximum shear to have a modifying effect on fatigue life. Figure 9 is a log–log plot of $\hat{\gamma} + \hat{\varepsilon}_n + \sigma_{no}/E$ versus life for Inconel 718-DA. The term $\hat{\gamma}$ is the maximum shear strain amplitude, $\hat{\varepsilon}_n$ is the strain amplitude normal to the maximum shear plane, and σ_{no} is the stress amplitude normal to the maximum shear plane. Observed correlation of biaxial-tension data to uniaxial data is nonconservative by greater than a factor of 4 in life. Damage mechanisms in

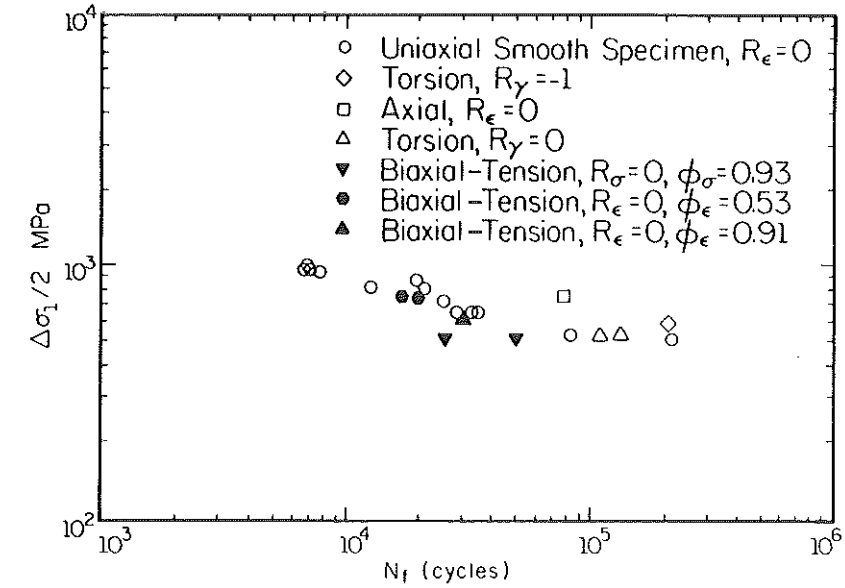

Fig 8 Principal stress amplitude correlation of Inconel 718-DA data

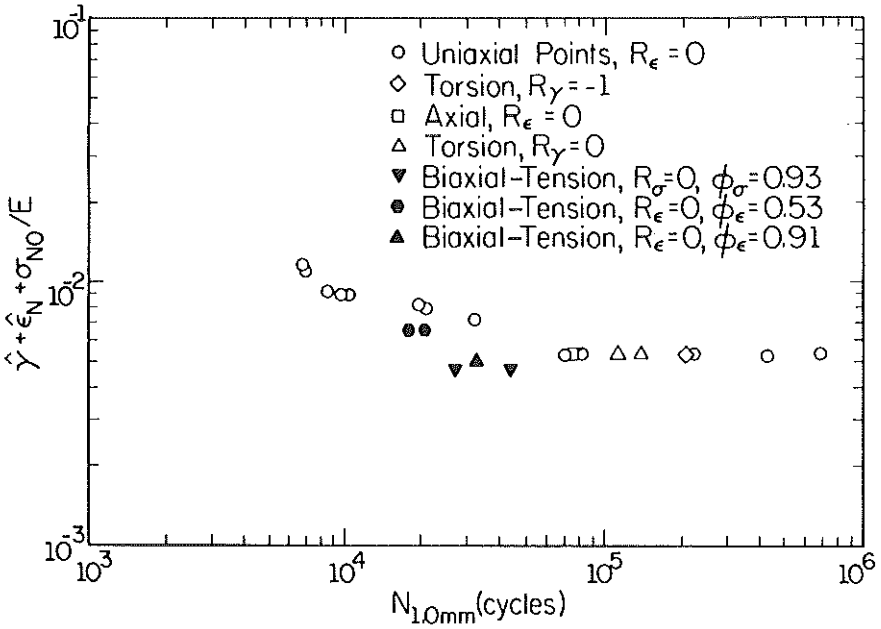

Fig 9 Shear strain based damage parameter correlation of Inconel 718-DA data

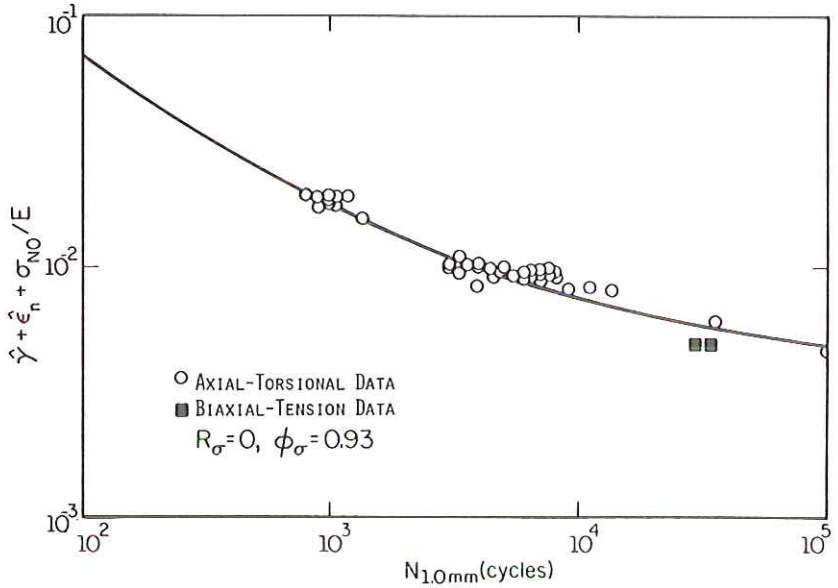

Fig 10 Shear strain based damage parameter correlation of Inconel 718 data

effect in the shear direction are not appropriate for this material at lives greater than 10^4 cycles.

Two biaxial-tension tests have been conducted on the coarser grained Inconel 718. These two points are plotted in Fig. 10 employing Socie's mean stress modified shear based damage parameter, with other strain quadrant II and IV biaxial test data (**22**)(**23**). Correlation for the previous life data is within a factor of 2. The plot represents a wide range of biaxial-tension ratios (ϕ_ε), load paths (i.e., proportional and non-proportional), and strain ratios (R_ε). Crack direction observations from prior research indicate the shear direction to be appropriate when formulating a damage criterion for this material (**23**)(**24**). This parameter was effective in correlating the $\phi_\varepsilon > 0$ as well as $\phi_\varepsilon < 0$ data, but insufficient $\phi_\varepsilon = +1$ data exist at this time to reach any firm conclusions. Surface crack observations of the biaxial-tension specimens do not provide conclusive evidence to support shear direction crack growth. The nearly equal biaxial-tension stress–strain state at the specimen surface does not dictate a specific shear direction on the specimen surface. Sectioning of the specimens and observation of growth into the specimen has revealed that shear crack growth occupied the major portion of the fatigue life (approximately 90 per cent). Using a shear based criterion, improved damage correlation was achieved for the coarse grained Inconel-718 in comparison to the fine grained alloy. This suggests that fatigue damage was not shear dominated for the finer grained material (Inconel 718-DA).

Considerable work remains to be done at lives less than 10^4 cycles in order to completely assess the effect of biaxial-tension stress ratio on fatigue life. The concept that fatigue damage occurs in a critical plane is appealing and should be incorporated in the analysis of multiaxial fatigue failure. Observation of physical damage may help define the important parameters in fatigue analysis for a given material. If a multiaxial theory successfully predicts the plane of fatigue initiation or crack growth, the appropriate parameters for fatigue life prediction will probably be included.

Conclusions

(1) A new test system was commissioned which allows strain controlled fatigue testing in stress or strain quadrants I and III.
(2) The biaxial-tension data generated for Inconel 718 and 718-DA indicate that $\phi = +1$ loadings are the most damaging for lives between 10^4 and 10^5 cycles.
(3) Coarse grained Inconel 718 biaxial-tension data were correlated with uniaxial and torsional baseline data within a factor of 2 in life using a shear based damage parameter. Observations of biaxial-tension cracking are required to verify whether it is appropriate to employ a shear based criterion for this material when loaded in stress quadrants I and II.
(4) The fine grained Inconel 718-DA biaxial-tension tests were best correlated with uniaxial and torsional baseline data by employing maximum principal stress as a damage criterion. Maximum principal strain and a shear based parameter provided poor correlation to the baseline uniaxial data. Again, future cracking observations will aid in the identification of the appropriate damage parameter.
(5) Present data indicate that the appropriate damage parameter for correlating biaxial-tension biaxial fatigue test data to strain quadrant II and IV data is material dependent.

Closure

A thorough understanding of the multiaxial fatigue behaviour of Inconel 718 has been attained since this paper was first presented in December 1985. Extensive crack monitoring and post-failure sectioning of specimens have revealed a consistent failure mode in all stress quadrants of shear crack nucleation followed by shear crack growth to failure for lives below 10^6 cycles. Interested readers should review Morrow (**25**).

Acknowledgements

Funding for this research was provided by the General Electric Corporation, Evandale, Ohio. Jess J. Comer provided expertise in the finite element analyses and assistance in conducting the tests. Technical guidance was pro-

vided by Dr Darrell F. Socie. Kent Elam expertly machined all specimens. Finally, June Kempka, Tammy Lawhead, and Suzanne Palmer are gratefully acknowledged for aiding in the preparation of this manuscript.

References

(1) KREMPL, E. (1974) The influence of state of stress on low-cycle fatigue of structural materials: a literature survey and interpretive report, *ASTM STP 549*, ASTM, Philadelphia, PA.

(2) BUNSHAH, R. F. (Editor) (1971) Measurement of mechanical properties, Part 1, *Techniques of Metals Research*, Vol. 5, Interscience, New York, pp. 126–197.

(3) GARUD, Y. S. (1981) Multiaxial fatigue: a survey of the state of the art, *J. Testing Evaluation*, **9**, 165–178.

(4) ZAMRIK, S. Y. (1985) Multiaxial fatigue low cycle fatigue testing, *Nonlinear Constitutive Relations for High Temperature Application – 1984*, NASA Conference Publication 2369, National Aeronautics and Space Administration, pp. 221–236.

(5) BROWN, M. W. and MILLER, K. J. (1973) A theory for fatigue failure under multiaxial stress–strain conditions, *Proc. Instn mech. Engrs*, **187**, 745–755.

(6) McDIARMID, D. L. (1972) *Failure criteria and cumulative damage in fatigue under multiaxial stress conditions*, PhD thesis, The City University, London, UK.

(7) BLASS, J. J. and FINDLEY, W. N. (1967) The influence of the intermediate principal stress on fatigue under triaxial stresses, *Mater. Res. Standardization*, **7**, 254–261.

(8) BUNDY, R. W. and MARIN, J. (1954) Fatigue strength of 14S-T4 aluminum alloy under biaxial stresses, *Proc. ASTM*, **54**, 755–768.

(9) PASCOE, K. J. and deVILLIERS, J. W. R. (1967) Low cycle fatigue of steels under biaxial straining, *J. Strain Analysis*, **2**, 117–126.

(10) HAVARD, D. G. (1970) *Fatigue and deformation of normalized mild steel subject to cyclic biaxial loading*, PhD thesis, University of Waterloo, Canada.

(11) HAVARD, D. G. and TOPPER, T. H. (1969) Biaxial fatigue of 1018 mild steel at low endurance, *Proceedings of the First International Conference on Pressure Vessel Technology*, Part II, pp. 1267–1277.

(12) HAVARD, D. G., WILLIAMS, D. P., and TOPPER, T. H. (1975) Biaxial fatigue of mild steel: data synthesis and interpretation, *Ontario Hydro. Res. Q.* (Second Quarter), 11–18.

(13) ANDREWS, J. M. H. (1972) *Biaxial high strain fatigue of an aluminum alloy*, PhD thesis, University of Bristol, UK.

(14) ELLISON, E. G. and ANDREWS, J. M. H. (1973) Biaxial cyclic high-strain fatigue of aluminum alloy RR58, *J. Strain Analysis*, **8**, 209–219.

(15) LOHR, R. D. and ELLISON, E. G. (1980) Biaxial high strain fatigue testing of 1Cr–Mo–V steel, *Fatigue Engng Mater. Structures*, **3**, 19–37.

(16) LOHR, R. D. and ELLISON, E. G. (1980) A simple theory for low cycle multiaxial fatigue, *Fatigue Engng Mater. Structures*, **3**, 1–17.

(17) LeFEBVRE, D., CHEBL, C., and KHAZZARI, E. (1984) Multiaxial high-strain fatigue of Grade 70, *Fatigue 84* (Proceedings of the 2nd International Conference on Fatigue and Fatigue Thresholds), Vol. 3, pp. 1695–1704.

(18) CHARVAT, I. M. H. and GARRETT, G. G. (1980) The development of a closed-loop servo-hydraulic test system for direct stress monotonic and cyclic crack propagation studies under biaxial loading, *J. Testing Eval.*, **8**, 9–17.

(19) HOSHIDE, T., TANAKA, K., and YAMADA, A. (1981) Stress-ratio effect of fatigue crack propagation in a biaxial stress field, *Fatigue Engng Mater. Structures*, **4**, 355–366.

(20) BROWN, M. W. and MILLER, K. J. (1985) Mode I fatigue crack growth under biaxial stress at room temperature, *Multiaxial Fatigue, ASTM STP 853*, ASTM, Philadelphia, PA, pp. 35–152.

(21) SOCIE, D. F., KURATH, P., and KOCH, J. L. (1988) A multiaxial LCF parameter, *Biaxial and Multiaxial Fatigue*, EGF 3 (Edited by BROWN, M. W. and MILLER, K. J.), Mechanical Engineering Publications, London, pp. 000–000. This volume.

(22) SOCIE, D. F., WAILL, L. A., and DITTMER, D. F. (1985) Biaxial fatigue of Inconel 718

including mean stress effects, *Multiaxial Fatigue, ASTM STP 853*, ASTM, Philadelphia, PA, pp. 463–481.

(23) BANNANTINE, J. A., and SOCIE, D. F. (1985) Observations of cracking behavior in tension and torsion low cycle in low cycle fatigue, presented at ASTM Conference 'Low Cycle Fatigue – Directions for the Future', Bolton Landing, NY, USA.

(24) KOCH, J. L. (1985) *Proportional and non-proportional biaxial fatigue of Inconel 718*, MSc thesis, Department of Mechanical and Industrial Engineering, University of Illinois at Urbana-Champaign, Urbana, IL, USA.

(25) MORROW, D. L. (1988) *Biaxial-tension fatigue of Inconel 718*, PhD thesis, Department of Mechanical and Industrial Engineering, University of Illinois at Urbana-Champaign, Urbana, IL, USA.